Electrical and deep-level characterization of $GaP_{1-x}N_x$ grown by gas-source molecular beam epitaxy

M. Kaneko[a] and T. Hashizume[b]
Research Center for Integrated Quantum Electronics, Hokkaido University, North 13, West 8, Kita-ku, Sapporo 060-8628 Japan

V. A. Odnoblyudov and C. W. Tu
Department of Electrical and Computer Engineering, University of California, San Diego La Jolla, California 92093-0407

(Received 20 December 2006; accepted 14 March 2007; published online 21 May 2007)

We have investigated electrical properties and deep levels of n-$GaP_{1-x}N_x$ ($x=0\%-0.62\%$) grown on (100) n-GaP substrates by gas source molecular beam epitaxy. The x-ray photoelectron spectroscopy results showed no significant effects on the chemical bonding status of the host Ga-P matrix by the incorporation of small amounts of N atoms. In the Raman spectra, the zone-edge GaP-like vibration was observed at 387 cm^{-1}, originating from alloy disorder or local distortion of the $GaP_{1-x}N_x$ lattice. The electrical properties of the $GaP_{1-x}N_x$ surfaces were characterized using a Schottky contact structure. An ideality factor of 1.10–1.15 and a Schottky barrier height of 1.1 eV were obtained from the current-voltage characteristics of $Ni/GaP_{1-x}N_x$ diodes, indicating good interface quality. The thermal admittance spectroscopy clearly detected the Si donor level with an activation energy of 84 ± 4 meV in GaP and $GaP_{1-x}N_x$. For the $GaP_{1-x}N_x$ samples, we observed deep levels probably associated with N-induced defects such as N-N pairs, N clusters, and an N-containing complexes.
 [DOI: 10.1063/1.2732451]

I. INTRODUCTION

The dilute nitride semiconductors, such as GaAsN, GaPN, and GaInPN, are promising materials for practical applications in optoelectronics,[1] such as visible-infrared LEDs,[2] the long-wavelength lasers[1,3,4] emitting at 1.3 and 1.55 μm, and photovoltaic devices,[5] due to their unique properties induced by N incorporation into a host III–V matrix. In fact, Odnoblyudov and Tu very recently reported[2] that amber GaPN LEDs, successfully fabricated on a transparent GaP (100) substrate, showed excellent stability of the electroluminescence wavelength on the driving current, as compared with commercially available AlInGaP LEDs.

The isoelectronic traps formed by incorporation of N into a host semiconductor matrix, interact with the conduction band of host semiconductor. Thus, the conduction band of III–V–N semiconductors is modified drastically, thereby leading to the large bowing of the band gap in III–V–N alloys as described in the band-anticrossing model.[6–8] In addition, the incorporation of N into conventional III–V compounds causes a large change in lattice constant, which is expected by Vegaard's law. In the case of $GaP_{1-x}N_x$, especially, it is theoretically predicted that only a 2% of N incorporation into the host GaP matrix makes its lattice constant to match that of Si.[9,10] Therefore, there is a possibility for integration of GaPN devices with Si devices utilizing the conventional Si technology.[11,12] For design and control of GaPN-based device structures, it is important to understand electrical properties of the GaPN surfaces, including junction characteristics, impurity and/or defect-induced electronic levels, and so on. Although structural and optical properties of $GaP_{1-x}N_x$ have extensively been studied,[7,13–21] there are only a few literatures[22–24] on their chemical and electrical properties.

In this paper, we characterize electrical properties and deep levels of n-type $GaP_{1-x}N_x$ alloy layers grown on (100) n-GaP substrates by gas-source molecular beam epitaxy (GSMBE), and compare them with those of a GaP layer.

II. EXPERIMENT

Figure 1 shows a schematic drawing of the $GaP_{1-x}N_x$ layer structure and the Schottky diode used in this study. The $GaP_{1-x}N_x$ wafers consisted of an n-$GaP_{1-x}N_x$ layer (0.5 μm) and an $n-$GaP buffer layer (0.3 μm) grown on n-GaP (100) substrates by GSMBE assisted by an rf-induced N plasma.[13] The substrate temperature was 510 °C for the growth of the $GaP_{1-x}N_x$ layers.[14] The Si doping concentration was designed to be 1×10^{17} cm^{-3} by controlling the temperature of the Si cell. The N concentration of the $GaP_{1-x}N_x$ layers was determined by x-ray diffraction. In this paper,

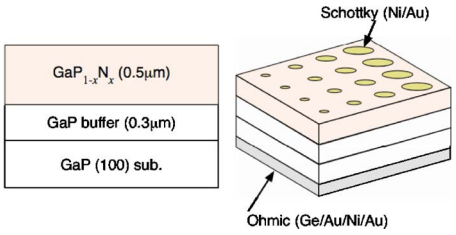

FIG. 1. (Color online) Schematic representation of the GaPN layered structure and the fabricated Schottky diode structure.

[a]Electronic mail: kaneko@rciqe.hokudai.ac.jp; URL: http://www.rciqe.hokudai.ac.jp/
[b]Electronic mail: hashi@rciqe.hokudai.ac.jp

$GaP_{1-x}N_x$/GaP samples with x=0, 0.25, 0.42, and 0.62% were used. These wafers were prepared at UCSD.

An ohmic contact consisting of a Ge/Au/Ni/Au layered structure was formed on the back side of a sample by electron beam deposition, followed by annealing at 380 °C for 5 min in an N_2 ambient. The $GaP_{1-x}N_x$ surface was cleaned with acetone and ethanol using an ultrasonic cleaner. Then the sample was rinsed with de-ionized water, and dried with nitrogen. In order to remove the native oxide from the $GaP_{1-x}N_x$ surface, the sample was dipped into 5% hydrochloric acid for 2 min. A circular shaped Schottky gate was formed on the $GaP_{1-x}N_x$ surface by depositing Ni/Au, as shown in Fig. 1. The diameter of the Schottky gate was chosen from 200 to 600 μm.

Chemical characterization of $GaP_{1-x}N_x$ alloy was performed using an x-ray photoelectron spectroscopy (XPS) system (Perkin-Elmer PHI 1600C) with a spherical capacitor analyzer and a monochromated Al $K\alpha$ radiation source ($h\nu$ =1486.6 eV). The energy scale was calibrated with the Au 4f spectrum ($h\nu$=84.0 eV), and the static electrification was compensated using the energy position of the C 1s core level in the C-H bond ($h\nu$=285.0 eV). The structural properties of $GaP_{1-x}N_x$ alloys were characterized by a Raman scattering spectroscopy system (Horiba Jobin Yvon T64000) using the 514.5 nm line of an Ar^+ laser. The 180° backscattering geometry was used throughout the experiments. The spectra of the (100) surfaces were taken in polarization configuration $x(y',y')\bar{x}$, where x denotes the [100] axis and y' denotes the [011] axis. The spectral resolution of the system was about 0.6 cm^{-1}. Electrical properties of fabricated Ni/$GaP_{1-x}N_x$ Schottky structures were examined by conventional current-voltage (I-V), capacitance-voltage (C-V), and thermal admittance spectroscopy[25] (TAS) measurements, using an HP4156A parameter analyzer and an HP4192A impedance analyzer. The sample temperature was swept from 30 to 300 K in a cryostat.

III. RESULTS AND DISCUSSION

A. XPS and Raman characterization

To investigate chemical and structural properties of the GaPN alloys basically, we carried out XPS and Raman measurements. Figure 2(a) shows the XPS P 2p core-level spectra obtained from the $GaP_{1-x}N_x$ (x=0, 0.25, and 0.62%) surfaces at an electron escape angle of 45°. Three peaks at 129.8, 130.5, and 135 eV, originating from the P $2p_{3/2}$, P $2p_{1/2}$ orbits in the Ga-P bond, and the P-oxide bond, respectively, were observed. The shapes and the energy positions of P 2p peaks remained unchanged with a slight variation in the N composition. A similar result was obtained for the Ga 3d spectra. Therefore, it is found that the slight incorporation of N less than 1% had no significant impact on the chemical bonding status of the host GaP matrix. The valence band (VB) spectra were shown in Fig. 2(b). The onset of the VB spectrum was the same for the three samples, indicating the same energy position of the VB maximum. On the other hand, a slight change was observed in the spectrum shapes by the addition of N into the host GaP matrix. The intensity of the broad peak at around 4 eV decreased with increasing

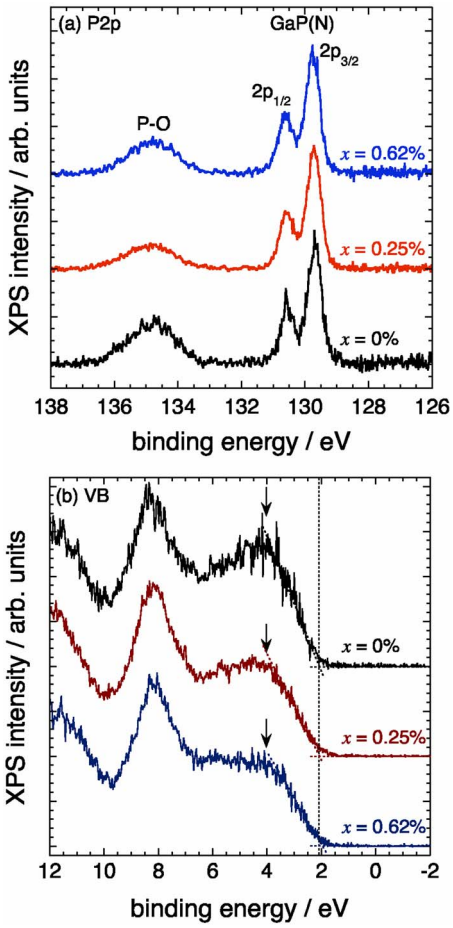

FIG. 2. (Color online) XPS spectra of (a) P 2p core-level and (b) valence band (VB) obtained from the $GaP_{1-x}N_x$ (x=0, 0.25, and 0.62%) surface with an electron escape angle of 45°.

the N composition. It may reflect modification of the density of states in VB, although the reason for this is not clear at present. A numerical calculation predicted a variation of the total valence charge densities for $GaP_{1-x}N_x$ with different N compositions.[26]

Figure 3(a) shows typical resonant Raman scattering spectra of the $GaP_{1-x}N_x$ alloys. There were three vibration components relating to a strong longitudinal-optic (LO) phonon mode at 405 cm^{-1}, a weak transverse-optic (TO) phonon mode at 366 cm^{-1}, and an additional mode (labeled as X) at 387 cm^{-1}, respectively. The spectra obtained were normalized by the intensity of the LO line for comparison. On the basis of the present symmetry configuration, the TO phonon vibration should be prohibited even for the GaP sample. However, we observed the TO peak even in the (100) GaP substrate. Thus, the incompleteness of scattering geometry and/or the imperfection of crystalline quality is probably responsible for a slight peak of the TO phonon. For $GaP_{1-x}N_x$, the X mode was observed at 387 cm^{-1}, and its intensity increased with the N composition. A similar scattering mode has already been reported in the GaAsP alloys[27,28] and $GaP_{1-x}N_x$ alloys.[17,19–21] Even though the origin of this mode is not known clearly, it has been expected that the compositional disorder (alloy disorder) or the N-induced lattice strain of $GaP_{1-x}N_x$ alloys can affect the host GaP LO phonon vi-

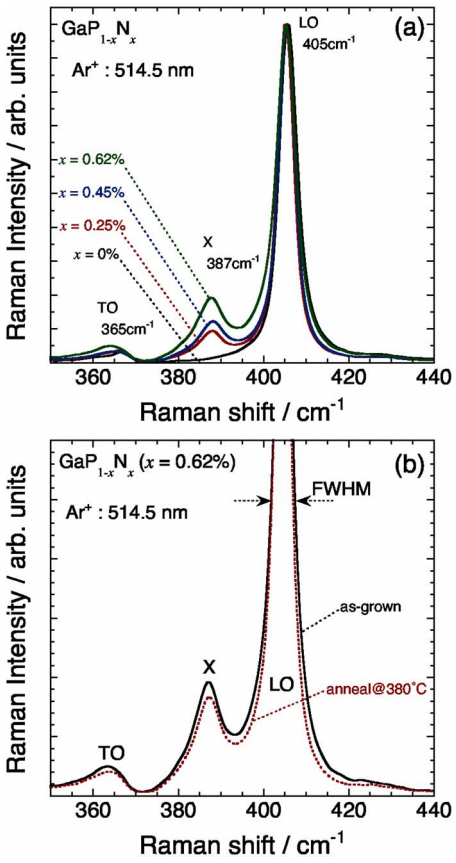

FIG. 3. (Color online) (a) Typical resonant Raman scattering spectra of the GaPN alloys measured at RT and (b) the spectra of the $GaP_{1-x}N_x$ (x =0.62%) alloy before and after annealing at 380 °C. The spectra obtained were normalized by the intensity of the LO line.

bration, leading to the activity of the X mode.[17,21] To investigate the influence of the annealing process for metallization of ohmic contact on the structural properties of $GaP_{1-x}N_x$ alloys, the Raman spectra were compared before and after the annealing process as shown in Fig. 3(b). After annealing at 380 °C for 2 min, the TO phonon peak and the X peak slightly decreased. In addition, we observed the narrowing of the full-width at half maximum (FWHM) at the LO phonon scattering line. The result indicates an improvement of the crystalline quality, probably due to the uniformity improvement of the N composition during the anneal.

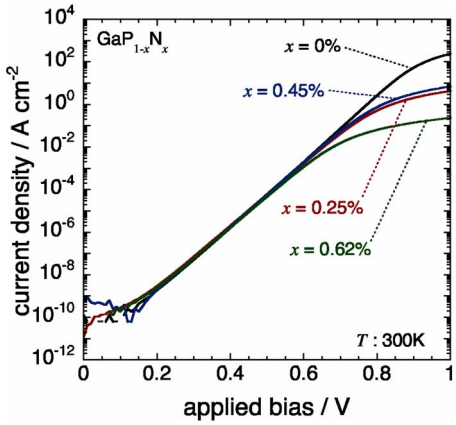

FIG. 4. (Color online) Typical forward I-V characteristics of a Ni/Au Schottky contact on the $GaP_{1-x}N_x$ (x=0, 0.25, 0.45, and 0.62%) surfaces at RT.

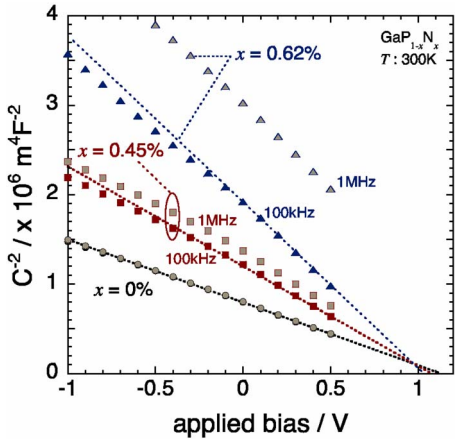

FIG. 5. (Color online) C^{-2}-V characteristics of Ni/Au Schottky contacts on the $GaP_{1-x}N_x$ surfaces at RT. The circle, rectangle, and triangle shapes represent the result of x=0%, 0.45%, and 0.62%, respectively. The circles, rectangles, and triangles represent the results for x=0%, 0.45%, and 0.62%, respectively.

B. *I-V* and *C-V* behavior of Ni/GaPN Schottky junctions

Figure 4 shows typical I-V characteristics of the Ni/$GaP_{1-x}N_x$ Schottky diodes measured at room temperature (RT). We observed good linearity in the ln(J)-V curves for 6–10 orders of magnitude in current, indicating that the simple thermionic-emission transport was dominant at the Schottky interfaces. The difference in saturation current at the higher bias is attributed to the difference in carrier concentration of the $GaP_{1-x}N_x$ layers. By applying the standard thermionic emission analysis to the experimental I-V curves, the ideality factors, n, are estimated to be 1.10–1.15 for all the $GaP_{1-x}N_x$ samples. We also found that the values of the Schottky barrier height (SBH) derived from the I-V plots was 1.1 eV, without depending on the N composition. These results indicated that relatively good Schottky contacts were fabricated on the $GaP_{1-x}N_x$ surfaces.

Figure 5 shows the C^{-2}-V plots for the GaP and $GaP_{1-x}N_x$ samples. From the plots at f=1 MHz, we estimated the densities of the shallow donors, N_D, in the GaP and $GaP_{1-x}N_x$ layers. Table I summarizes the evaluated values of the ideality factor, SBH, and shallow donor density of GaP and $GaP_{1-x}N_x$ with different N composition. In spite of the fact that we used the same Si doping condition during the epitaxial growth, the shallow donor density decreased with

TABLE I. Summary of electrical characteristics in Ni/$GaP_{1-x}N_x$ (x=0%, 0.45%, and 0.62%) Schottky diodes.

x in $GaP_{1-x}N_x$ (%)	n value[a]	SBH[a] (eV)	N_D [b] (cm^{-3})
0	1.11	1.10	1.9×10^{17}
0.45	1.12	1.09	9.0×10^{16}
0.62	1.15	1.08	6.0×10^{16}

[a]Derived from I-V.
[b]Derived from C-V.

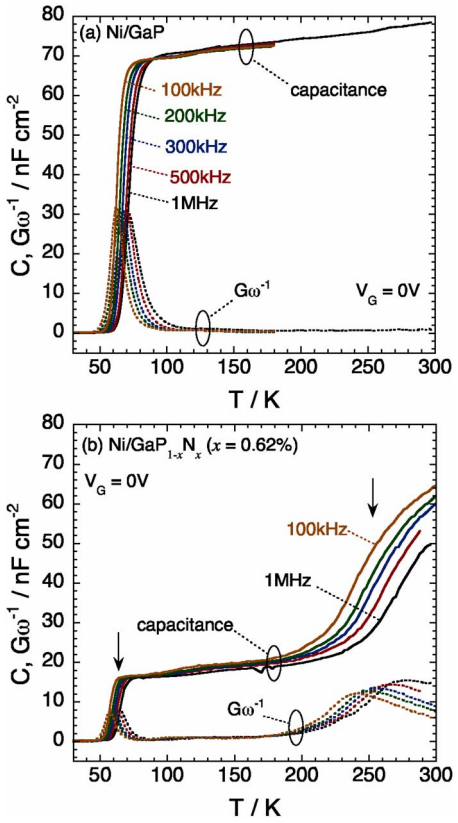

FIG. 6. (Color online) Typical thermal admittance spectra taken from the (a) Ni/GaP and (b) Ni/$GaP_{1-x}N_x$ (x=0.62%) interface at a temperature ranging from 30 to 300 K. The measurement was done at a frequency of 1 MHz, 500 kHz, 300 kHz, 200 kHz, and 100 kHz, respectively, with an ac signal rms value of 20 mV.

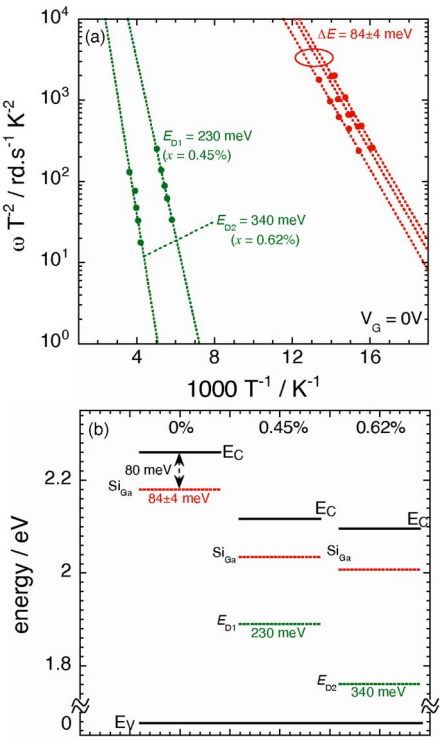

FIG. 7. (Color online) (a) Thermal emission rate related to each conductance peak as a function of reciprocal temperature and (b) the energy position of the levels detected in the Ni/$GaP_{1-x}N_x$ (x=0%, 0.45%, and 0.62%) alloys.

increasing the N composition in the $GaP_{1-x}N_x$ layers. A similar reduction of electron concentration was reported by Furukawa *et al.*[24] in the S and Te-doped $GaP_{1-x}N_x$ layers grown by rf-MBE. They suggest that such reduction of the carrier concentration could arise from the N-impinging desorption of the dopants from the surface during growth, or the electron capture by N-related deep levels. The frequency dispersion of capacitance obviously appeared in the *C-V* characteristics for the $GaP_{1-x}N_x$ samples, indicating the existence of deep levels in the $GaP_{1-x}N_x$ alloys.

C. TAS study

To investigate shallow and deep levels in the $GaP_{1-x}N_x$ layers, we employed TAS measurements in the GaPN samples. Figure 6(a) shows admittance (capacitance and conductance corrected by the angular frequency) spectra from a Ni/GaP diode at a temperature ranging from 30 to 300 K. The measurements were performed at a modulation frequency from 100 kHz to 1 MHz. The bias voltage was 0 V. For the GaP sample, the capacitance curves showed nearly plateau behavior for each frequency at temperatures ranging from 100 to 300 K. Then, the capacitance suddenly decreased at the temperature around 60 K. At the same temperature, the conductance curves showed the maximum values. Figure 6(b) shows admittance spectra taken from a Ni/$GaP_{1-x}N_x$ (x=0.62%) Schottky diode. In contrast to the capacitance curves of the Ni/GaP diode in Fig. 6(a), there were two inflection points for the Ni/$GaP_{1-x}N_x$ diode, as indicated by the arrows in Fig. 6(b). The corresponding two peaks were observed in the conductance curves. This result exhibits that the $GaP_{1-x}N_x$ alloy has at least two trap levels.

At the temperature in which a conductance maxima appears at each frequency, a thermal emission rate of the trap level, e_n^t, is expressed by the following equations:[25]

$$e_n^t(T_m) = \omega = \sigma_{\text{th}} N_C v_{\text{th}} \exp\left(-\frac{E_a}{kT_m}\right) = \sigma_{\text{th}} N_{C0} v_{\text{th}0} T_m^2 \exp\left(-\frac{E_a}{kT_m}\right), \quad (1)$$

where ω is the angular frequency, T_m is the temperature at which the maximum of conductance appears, σ_{th} and E_a are thermal cross section and activation energy of a trap level, N_C is the effective density of states at the conduction band minimum, v_{th} is the thermal velocity, and k is the Boltzmann constant. From Arrhenius plots of the temperature-corrected angular frequency, we can estimate activation energies of trap levels.

Figures 7(a) and 7(b) show the Arrhenius plots of the temperature-corrected emission rates of the trap levels and the energy level diagrams for the $GaP_{1-x}N_x$ alloy systems, respectively. For Fig. 7(b), we assumed a constant energy level for the valence band maximum in the $GaP_{1-x}N_x$ alloy system, according to the BAC model. Then the energy of the conduction band minimum is simply determined by the band gap energy of $GaP_{1-x}N_x$ in the literatures.[7,13] As shown in Fig. 7(a), the trap level with a thermal activation energy of

about 84±4 meV exists in all the samples. This value is very close to the ionization energy of a Si donor occupying the Ga site in the GaP lattice.[29–31] No pronounced change in the activation energy of the Si donor was observed in the $GaP_{1-x}N_x$ alloys. Furukawa *et al.*[24] also reported almost the same activation energy for the S dopant in $GaP_{1-x}N_x$ ($x=0\%-1.9\%$).

In addition to the Si donor level, we detected deeper trap levels for the $GaP_{1-x}N_x$ alloys, labeled by E_{D1} and E_{D2} in Fig. 7(b). These levels have a tendency to become deeper in energy with an increasing N composition. Again, these levels were not detected in GaP but in $GaP_{1-x}N_x$, indicating that the origin of the levels is related to defects induced by the incorporation of N atoms. From the detailed PL analysis, Buyanova *et al.*[18] suggested the existence of deep levels related to N-N pairs and/or N clusters in the $GaP_{1-x}N_x$ alloy. Furukawa *et al.*[24] pointed out the possibility for complex defects consisting of shallow impurities and N atoms. From deep level transient spectroscopy measurements in the GaAsN alloy, in addition, Johnston and Kurtz[32] very recently detected the deep trap whose density correlated with both the N composition and the electron concentration. Since we observed the reduction of the Si donor density (Table I) and the peak intensity of conductance for the Si donor in the $GaP_{1-x}N_x$ alloy [Fig. 6(b)], the deep levels detected may compensate the Si donor. Another possibility is that the deep levels observed may be related to complex defects with N and Si atoms. To see properties of the deep levels in detail, further investigations are necessary.

IV. CONCLUSION

Electrical properties and deep levels of $GaP_{1-x}N_x$ ($x=0\%-0.62\%$) grown by gas-source molecular beam epitaxy were investigated using the Ni Schottky contact structures. The XPS analysis showed that no significant effects on the chemical bonding status of the host Ga-P matrix by the incorporation of small amounts of N atoms. We observed similar Raman spectra of the $GaP_{1-x}N_x$ layers to those reported in the literatures. The Schottky *I-V* characteristics provided the ideality factors of 1.10–1.15 and a barrier height of 1.1 eV, indicating good interface quality between the metal and $GaP_{1-x}N_x$. From the capacitance-voltage measurement, we found the reduction of the shallow donor density with the N composition in the $GaP_{1-x}N_x$ layers. The thermal admittance spectroscopy clearly detected the Si donor level with an activation energy of 84 meV in GaP and $GaP_{1-x}N_x$. For the $GaP_{1-x}N_x$ samples, we observed deep levels probably associated with N-induced defects such as N-N pairs, N clusters, and N-containing complexes.

[1] C. W. Tu, J. Phys. Condens. Matter **13**, 7169 (2001).
[2] V. A. Odnoblyudov and C. W. Tu, J. Vac. Sci. Technol. B **24**, 2202 (2006).
[3] Y. Q. Wei, Y. Fu, D. Wang, P. Modh, P. O. Hedekvist, Q. F. Gu, M. Sadeghi, S. M. Wang, and A. Larsson, Appl. Phys. Lett. **87**, 081102 (2005).
[4] J. A. Gupta, G. I. Sproule, X. Wu, and Z. R. Wasilewski, J. Cryst. Growth **291**, 86 (2006).
[5] J. F. Geisz and D. J. Friedman, Semicond. Sci. Technol. **17**, 769 (2002).
[6] W. Shan, W. Walukiewicz, J. W. Ager III, E. E. Haller, J. F. Geisz, D. J. Firedman, J. M. Olson, and S. R. Kurtz, Phys. Rev. Lett. **82**, 1221 (1999).
[7] W. Shan, W. Walukiewicz, K. M. Yu, J. Yu, J. W. Ager III, E. E. Haller, H. P. Xin, and C. W. Tu, Appl. Phys. Lett. **76**, 3251 (2000).
[8] I. A. Buyanova, M. Izadifard, A. Kasic, H. Arwin, W. M. Chen, H. P. Xin, Y. G. Hong, and C. W. Tu, Phys. Rev. B **70**, 085209 (2004).
[9] K. Momose, H. Yonezu, Y. Fujimoto, Y. Furukawa, Y. Motomura, and K. Aiki, Appl. Phys. Lett. **79**, 4151 (2001).
[10] M. Izadifard, J. P. Bergman, I. Vorona, W. M. Chen, I. A. Buyanova, A. Utsumi, Y. Furukawa, S.-Y. Moon, A. Wakahara, and H. Yonezu, Appl. Phys. Lett. **85**, 6347 (2004).
[11] H. Yonezu, Y. Furukawa, H. Abe, Y. Yoshikawa, S.-Y. Moon, A. Utsumi, Y. Yoshizumi, A. Wakahara, and M. Ohtani, Opt. Mater. **27**, 799 (2005).
[12] Y. Furukawa, H. Yonezu, Y. Morisaki, S.-Y. Moon, S. Ishiji, and A. Wakahara, Jpn. J. Appl. Phys., Part 2 **45**, L920 (2006).
[13] W. G. Bi and C. W. Tu, Appl. Phys. Lett. **69**, 3710 (1996).
[14] V. A. Odnoblyudov and C. W. Tu, J. Vac. Sci. Technol. B **23**, 1317 (2005).
[15] L. Bellaiche, S.-H. Wei, and A. Zunger, Phys. Rev. B **56**, 10233 (1997).
[16] P. R. C. Kent and A. Zunger, Phys. Rev. B **64**, 115208 (2001).
[17] I. A. Buyanova, W. M. Chen, E. M. Goldys, H. P. Xin, and C. W. Tu, Appl. Phys. Lett. **78**, 3959 (2001).
[18] I. A. Buyanova, G. Y. Rudko, W. M. Chen, H. P. Xin, and C. W. Tu, Appl. Phys. Lett. **80**, 1740 (2002).
[19] S. Yoon, M. J. Seong, J. F. Geisz, A. Duda, and A. Mascarenhas, Phys. Rev. B **67**, 235209 (2003).
[20] I. A. Buyanova, M. Izadifard, I. G. Ivanov, J. Birch, W. M. Chen, M. Felici, A. Polimeni, M. Capizzi, Y. G. Hong, H. P. Xin, and C. W. Tu, Phys. Rev. B **70**, 245215 (2004).
[21] S. Yoon, J. F. Geisz, S.-H. Han, A. Mascarenhas, M. Rübhausen, and B. Schulz, Phys. Rev. B **71**, 155208 (2005).
[22] J. F. Geisz, R. C. Reedy, B. M. Keyes, and W. K. Metzger, J. Cryst. Growth **259**, 223 (2003).
[23] Y. G. Hong, A. Nishikawa, and C. W. Tu, Appl. Phys. Lett. **83**, 5446 (2003).
[24] Y. Furukawa, H. Yonezu, A. Wakahara, Y. Yoshizumi, Y. Morita, and A. Sato, Appl. Phys. Lett. **88**, 142109 (2006).
[25] J. Barbolla, S. Dueñas, and L. Bailón, Solid-State Electron. **35**, 285 (1992).
[26] F. Benkabou, J. P. Becker, M. Certier, and H. Aourag, Superlattices Microstruct. **23**, 453 (1998).
[27] D. Schmeltzer and R. Beserman, Phys. Rev. B **22**, 6330 (1980).
[28] C. Ramkumar, K. P. Jain, and S. C. Abbi, Phys. Rev. B **54**, 7921 (1996).
[29] H. C. Montgomery and W. L. Feldmann, J. Appl. Phys. **36**, 3228 (1965).
[30] P. J. Dean, C. J. Frosch, and C. H. Henry, J. Appl. Phys. **39**, 5631 (1968).
[31] A. A. Kopylov and A. N. Pikhtin, Solid State Commun. **26**, 735 (1978).
[32] S. W. Johnston and S. R. Kurtz, J. Vac. Sci. Technol. A **24**, 1252 (2006).